Observation of pH-Dependent Back-Electron-Transfer Dynamics in Alizarin/TiO_2 Adsorbates: Importance of Trap States

V. V. Matylitsky, M. O. Lenz, and J. Wachtveitl*

Institute of Physical and Theoretical Chemistry, Johann Wolfgang Goethe-University Frankfurt/M, Max-von-Laue-Strasse 7, D-60438 Frankfurt/M, Germany

Received: January 27, 2006; In Final Form: March 8, 2006

The dependence of the interfacial electron transfer in alizarin-sensitized TiO_2 nanoparticles on the sample pH has been examined via transient absorbance spectroscopy in the visible spectral region (443−763 nm). Excitation of the alizarin/TiO_2 system with visible pump pulses ($\lambda_{exc} = 500$ nm) leads to a very fast electron injection ($\tau_{inj} < 100$ fs) over a wide pH range. Back electron transfer shows complicated multiphasic kinetics and strongly depends on the acidity of the solution. The strong dependence of back-electron-transfer dynamics on the ambient pH value is explained by a Nernstian-type change in the semiconductor band energy. Indeed, a variation of pH values over 7 units leads to a ∼0.42 eV change of the conduction band edge position (i.e., the nominal free energy of the electron in the electrode). Assuming a pH-independent redox potential of the dye, this change was sufficient to push the system to a condition where direct photoinitiated electron injection to intraband gap surface states could be investigated. The existence of an electron-transfer pathway via surface trap states is supported by the similarity of the observed back-electron-transfer kinetics of alizarin/TiO_2 at pH 9 and alizarin/ZrO_2 reported in earlier work (*J. Phys. Chem. B* **2000**, *104*, 8995), where the conduction band edge is approximately 1 eV above the excited state of the dye. The influence of surface trap states on interfacial electron transfer has been studied, and a detailed analysis of their population, depopulation, and relaxation kinetics is performed. Therefore, alizarin adsorbed on the surface of TiO_2 nanoparticles is an ideally suited system, where pH-dependent investigations allow a detailed study of the electron dynamics in trap states of TiO_2 nanoparticles.

Introduction

Electron transfer (ET) between molecular adsorbates and semiconductor nanomaterials has attracted much interest during the past few years. The interest is based on many applications such as water purification,[1] solar energy conversion,[2,3] and molecular electronics,[4] where interfacial ET plays a key role. The interfacial-electron-transfer process can be divided into two parts: *forward* and *back* electron transfer. Optical excitation of the sensitizing dye to its excited state above the conduction band edge of the semiconductor nanoparticles initiates electron injection (forward electron transfer (FET)) on a fast or ultrafast time scale.[5−13] After injection, the electron may recombine with the dye cation (back electron transfer (BET)) on a time scale of femtoseconds up to microseconds.[14−17] The wide time range of BET normally is explained by strong contributions of semiconductor effects such as charge trapping and spatial diffusion.[11,18,19] From the comparison of experimental results with theoretical predictions, it has been concluded that the reaction of BET is mainly governed by the energy redistribution of trapped electrons rather than by spatial diffusion.[19]

According to Marcus theory, the main parameters for the ET rate are the electronic coupling between the electron-donating and electron-accepting states and the standard Gibbs energy difference $\Delta G = E_{CB} - E(S^+/S^*)$ between the donor and acceptor states (see Scheme 1), i.e., the "driving force" of the reaction.[20,21] Another very important parameter for interfacial ET is the density of the accepting state in the semiconductor.[20,22−24] Up to now, mainly interfacial ET to high densities of accepting states in the conduction band has been studied. Only a few publications are available where discrete surface states were directly involved in ET processes. These studies focus on the dynamics of interfacial ET from dyes to insulating semiconductor nanoparticles such as ZrO_2, where the conduction band edge is significantly higher than the relevant excited state of the sensitizing dye. The appearance of a fast FET reaction for a dye/ZrO_2 system in the near-infrared region has been reported for the first time by Ellingson et al.[25] The detailed investigation of the interfacial FET in dye/ZrO_2 systems has been done using transient absorbance spectroscopy utilizing visible probe wavelengths[8] and time-resolved absorption polarization spectroscopy.[26] Ghosh et al. used time-resolved emission spectroscopy to investigate the effect of surface modification on the ET dynamics into the surface states of ZrO_2 nanoparticles sensitized by quinizarin and its derivatives.[27] In all of these studies the importance of the surface states for interfacial ET has been emphasized.

An alternative way to change the relative energies of the electronic states participating in ET, i.e., the driving force of the reaction, is to tune the conduction band position by varying the ambient pH value of the sample. pH variation leads to a Nernstian-type change in the semiconductor band energies of metal oxide semiconductors:[11,28−30]

$$E_{CB}(\mathrm{pH}) = E_{CB}(\mathrm{pH}\ 0) - 0.059 \times \mathrm{pH}\ [\mathrm{eV\ vs\ NHE}]$$

This implies that the conduction band edge moves to a more negative potential with increasing pH. With the assumption that

* To whom correspondence should be addressed. E-mail: wveitl@theochem.uni-frankfurt.de. Fax: +49 69 798 29709.

10.1021/jp060588h CCC: $33.50
Published on Web 04/06/2006

the redox potential of the sensitizing dye is unchanged with pH, changes in the ET dynamics should directly reflect the role of the driving force and the density of accepting states (ref 11 and references therein). It should be noted here that several studies show the appearance of an unusual pH dependence of the dye oxidation potential upon coupling with nanocrystalline TiO_2 despite its pH independence in solution.[31,32] It has been shown that, in dye/semiconductor systems with appropriate dye structure and electrolyte composition, the redox potential of the dye tends to follow the changes of the semiconductor potential.[31] Moreover, the authors proposed this effect to explain the pH-independent rate of the back ET[32] previously observed by Yan and Hupp for the covalently bound dyes.[29] On the other hand, the decoupling of the ET kinetics from the pH-variable energetics was interpreted in terms of sequential electron-transfer−proton-transfer processes, where electron addition induces the intercalation of charge-compensating cations.[29,33]

In this work we report investigations of alizarin-sensitized TiO_2 colloid nanoparticles in solution at pH 2 and 9 by means of steady-state and subpicosecond time-resolved spectroscopic methods. Alizarin as a sensitizing dye for TiO_2 nanoparticles is especially well suited, since according to the results of quantum-chemical calculations[13,34] the excited state is positioned near the TiO_2 semiconductor band edge. Indeed, fast electron injection from photoexcited states of alizarin directly to surface trap states of the colloid has been observed in basic aqueous solution. Moreover, the results of transient absorbance measurements for the alizarin/TiO_2 system at pH 9 are in agreement with the results obtained by the same method for alizarin/ZrO_2 reported by Huber et al.[8] A detailed description of the processes following the photoexcitation of alizarin/TiO_2 in solution at different pH values is derived from analyses of the amplitude spectra obtained as a result of the fitting procedure and on the basis of a discussion published earlier.[8] Additionally, the peculiar properties and dynamics of free alizarin in the electronically excited state in aqueous solution will be presented.

Experimental Section

Materials. Colloidal nanoparticles of TiO_2 in acidic solution (pH $\approx$ 2) were prepared as described earlier.[35] The average diameter of the TiO_2 particles was about 15 nm, as measured by dynamic light scattering. To allow investigations with the samples at pH > 3, the stabilizing agent poly(vinyl alcohol) (PVA) (Fluka, 0.1% solution, $M_w = 61000$) for TiO_2 sol was added to the acidic solution. Then the pH was raised by removing the HCl via treatment with Dowex MR-3 mixed bed ion-exchange resin supplied by Sigma-Aldrich. After approximately 30 min of treatment TiO_2 nanoparticles in almost neutral (pH 6) solution were obtained. The adjustment of the final pH was done by adding NaOH.

Since alizarin (purity 97%, Aldrich) is poorly soluble in water, we used ethanol as the solvent for the dye and then added this solution to the aqueous colloidal solution. Weak solubility of alizarin in water guaranties high efficiency of coupling of the dye to the TiO_2 nanoparticle surface.

All chemicals were at least reagent grade and used as supplied by the vendor.

Stationary Spectroscopy. Absorption measurements were performed using 1 × 1 cm fused silica cuvettes in an Analytik Jena S 100 spectrometer. To ensure that no photoinduced accumulation of photoproducts appears, absorption spectra were taken before and after the time-resolved measurements. Fluorescence spectra were measured utilizing a Varian Cary Eclipse fluorometer. Concentrations: 8×10^{-2} mM alizarin (in the case of coupled and uncoupled systems) and 0.25 g/L colloidal TiO_2 in water-ethanol mixture were used for the steady-state characterization. Higher concentrations (1.5×10^{-1} mM, 0.45 g/L) for the alizarin/TiO_2 system at pH 2 were used to achieve comparable optical density for the samples at $\lambda_{exc} = 490$ nm.

CHART 1: Chemical Structure of Alizarin (a) and Its Monoanionic (b) and Dianionic (c) Forms (Reported in Ref 40)

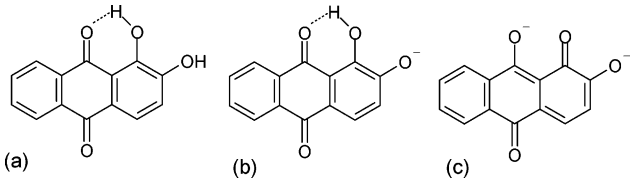

Time-Resolved Spectroscopy. Since details of the employed femtosecond spectrometer have been described elsewhere,[36,37] only a brief description will be given here. The spectrometer is based on a CLARK CPA 2001 laser/amplifier system. Part of the pulses stemming from this source are converted to pulses with the desired excitation wavelength utilizing a home-built noncollinear optical parametric amplifier (NOPA),[38] resulting in an excitation energy between 200 and 700 nJ. These pulses are focused down to a diameter of 100 μm inside the sample. To avoid multiple excitation of the same probing volume, the cuvette (path length 1 mm, fused silica) was mounted on an $x-y$ translation stage[39] and moved with the appropriate speed. To compensate the 1 mm cell path length, a higher sample concentration in comparison with cw measurements was used. Both free alizarin (1 mM) and the coupled system (1 mM alizarin, 12 g/L TiO_2) were solved in a water−ethanol mixture (4:1, v/v). The samples were probed with single-filament white light generated in an oriented sapphire substrate of 2 mm thickness. The white light continuum pulses were dispersed by two VIS spectrometers (signal and reference) and recorded with two 42-segment diode arrays. A spectral range for probing from 443 to 763 nm could be realized with this setup, providing signal-to-noise ratios up to $\sim 10^4$.

Before a complete fitting analysis, the experimental data were corrected for the coherent signal and group velocity dispersion. A Marquardt downhill algorithm was used for fitting the experimental data by n exponential decays simultaneously, while the amplitudes for each kinetic component are wavelength-dependent fitting parameters.[8,9,36]

Results

Steady-State Spectroscopy. For the study of the pH dependence of interfacial electron transfer it is important to know both the ground- and excited-state properties of the investigated system for different pH values. Miliani et al.[40] have reported pH-dependent absorption and fluorescence spectra of alizarin in a water−dioxane mixture (2:1, v/v) in the pH range of 2−14. A red shift of the absorption spectra was observed with increasing pH and explained by the formation of three distinct species. These species were identified as the neutral (acidic solutions), the monoanionic (neutral and moderately basic solutions), and the dianionic (basic solutions) alizarin forms (see Chart 1). All three species are weakly fluorescent with fluorescence quantum yields of $\Phi_F = 10^{-4}-10^{-3}$.[40] The situation is complicated due to a double emission arising through intramolecular excited-state proton transfer (ESPT), which occurs from the phenolic hydroxyl to the carbonyl oxygen (see Chart 1), accompanied by large changes in the geometry of the molecule.[41]

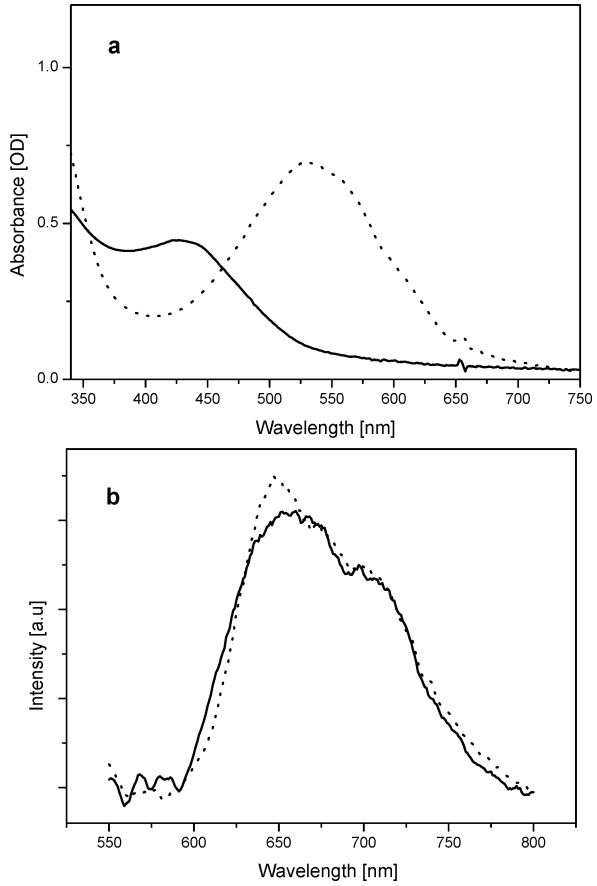

Figure 1. (a) Absorption and (b) normalized fluorescence spectra of free alizarin (8×10^{-5} M) in an ethanol−water mixture at pH 2 (solid line) and pH 9 (dotted line). The emission spectra were obtained after excitation of the main absorption band of the samples with pH 2 and 9 at 427 and 530 nm, respectively.

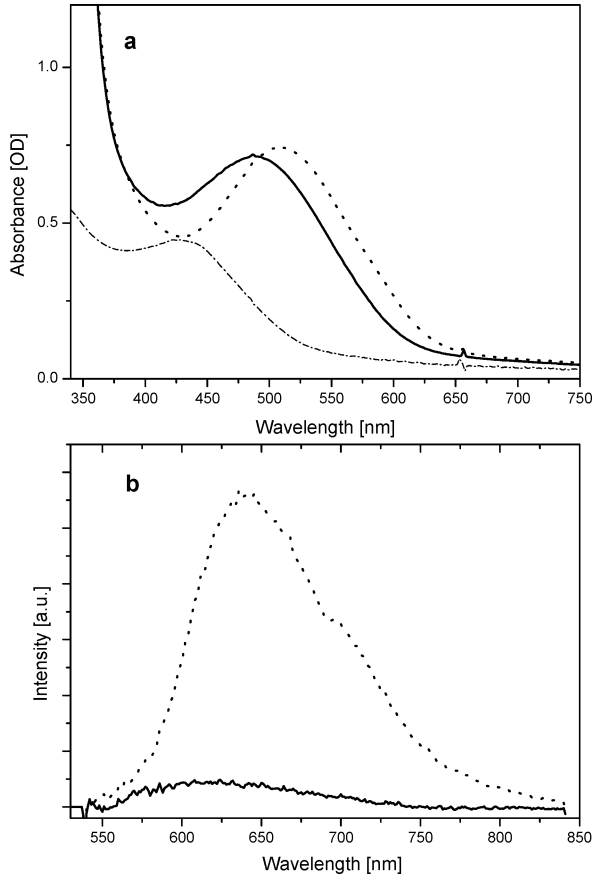

Figure 2. (a) Absorption and (b) fluorescence spectra of alizarin coupled to TiO_2 colloids in an ethanol−water mixture at pH 2 (concentrations: alizarin, 1.5×10^{-4} M; TiO_2, 0.45 g/L) (solid line) and pH 9 (concentrations: alizarin, 8×10^{-5} M; TiO_2, 0.25 g/L) (dotted line), in comparison with the free dye (dashed−dotted line). The emission spectra were obtained after excitation at 490 nm. Note: A higher concentration at pH 2 was used to achieve comparable optical densities for the samples at $\lambda_{exc} = 490$ nm.

We have carried out steady-state absorption and emission studies of both alizarin and alizarin-sensitized TiO_2 nanoparticles in an ethanol−water mixture at pH values of 2 and 9. Figure 1a shows the absorption spectra of free alizarin in ethanol−water at pH 2 and 9 which exhibit peaks at 427 and 532 nm, respectively. From Figure 1a it is obvious that with rising pH a new species is formed in solution absorbing at 532 nm, which can be ascribed to the monoanionic form of alizarin.[40] The maximum of the main absorption band of the anionic form is red-shifted compared to that of the neutral form (∼105 nm) and even to that of the charge-transfer complex of the coupled dye/nanoparticle system (∼20 nm). Similar observations have been described by Rath et al. for quinizarin and its derivatives.[27]

Under the experimental conditions used, only a very weak fluorescence from alizarin in the ethanol−water mixture could be observed. Moreover, the intensity of the fluorescence band is almost pH-independent. Figure 1b shows normalized alizarin fluorescence spectra at pH 2 and 9 measured after excitation of the main absorption band at 427 and 530 nm, respectively. The region of the spectra below 600 nm has to be considered with caution, since here the fluorescence was affected by strong sample reabsorption and scattered light. We did not observe any emission dependence on the pH, and the reported fluorescence spectra can be assigned to the red band of the alizarin dual fluorescence from a tautomeric form.[40,41] In polar solvents, such as water, the barrier to ESPT is lowered[41] and the molecules can decay radiatively mainly from the tautomeric, proton-transferred state.[8,41−43]

Figure 2a shows the absorption spectra of alizarin-sensitized TiO_2 nanoparticles at different pH values in comparison with the spectrum of free alizarin. The large shifts of ∼59 nm at pH 2 and ∼85 nm at pH 9 of the absorption maximum upon complexation with TiO_2 indicate a very strong electronic coupling between alizarin and the semiconductor surface and the appearance of a new ligand-to-metal charge-transfer absorption band.[8,44] Although the absorption of free alizarin shows a strong dependence on the solution pH (see Figure 1a), the pH dependence upon coupling is much weaker. This implies that mainly the neutral form is present in the coupled systems over the entire investigated pH range. Indeed, absence of a deprotonation of an alizarin-type dye adsorbed on a nanoporous TiO_2 film has been observed over a wide pH range. This property was used for anion sensing employing the molecular receptor alizarin complexone adsorbed onto a nanocrystalline TiO_2 film without the use of buffering solutions.[45] The minor difference in the position of the absorption maxima at different pH values can be explained by the appearance of a small fraction of the alizarin anion at high pH values. Although it has been reported that dyes which are strongly bound to a nanoparticle surface in aqueous solution can be desorbed at pH higher than 8.5,[31] we observed that the main fraction of alizarin stays coupled even at pH 9. Both the results of dialysis experiments [we did not observe any significant changes in the absorption spectrum and coupled alizarin/TiO_2 system at pH 9 after 10 h of dialysis of

the sample using regenerated cellulose dialysis tubing (MWCO 1000, Carl Roth GmbH)] and the red-shifted absorption (~20 nm) of the deprotonated alizarin form at pH 9 in comparison to the ligand-to-metal charge-transfer absorption band with the same pH (Figures 1a and 2a) can be considered as proof for coupling of alizarin with TiO_2 nanoparticles even in a basic solution. However, to ensure that the main fraction of the dye molecules is permanently bound to the nanoparticle surface during the experiment, we limited our studies to pH 9.

In contrast to the results of fluorescence measurements for the free alizarin described above, the fluorescence quantum yield of the alizarin/TiO_2 systems increases with the pH of the solution. The fluorescence spectra of the coupled alizarin/TiO_2 systems in Figure 2b show a ~15 times higher fluorescence intensity at pH 9 than at pH 2. It is necessary to note that the concentration of alizarin and TiO_2 nanoparticles was approximately 2 times higher in the case of pH 2. We used a higher concentration to have comparable optical densities (see Figure 2a) for the samples (pH 2 and 9) at the excitation wavelength ($\lambda_{exc} = 490$ nm). Moreover, fluorescence from alizarin coupled to the TiO_2 nanoparticle surface in an ethanol−water mixture at pH 9 is also stronger than fluorescence of free alizarin in the same solvent in the pH range between 2 and 9. The observation is in good agreement with the obtained increase in fluorescence intensity upon alizarin adsorption at the ZrO_2 surface, where no electron transfer from the excited state of the dye to the semiconductor bulk states was expected.[8] Therefore, this fact strongly supports the similarity of the processes occurring in alizarin/TiO_2 at high pH and in alizarin/ZrO_2 systems and corroborates the assumption that at pH 9 the bottom of the conduction band of the TiO_2 nanoparticles is above the S_1 energy level of the excited state of alizarin. Thus, the alizarin/TiO_2 system at high pH can be regarded as a very promising model for the investigation of interfacial electron injection into the intraband surface states.

Transient Absorbance Measurements of Free Alizarin. The excited-state dynamics of free alizarin in ethanol and in a water−ethanol (4:1, v/v) mixture have been studied using transient absorbance spectroscopy. The sample was excited with 490 nm laser pulses (pulse duration ~30 fs) and probed in the wavelength region between 440 and 750 nm. The excited state of alizarin was subjected to several earlier investigations.[8,15] We reported an excited-state lifetime of alizarin in methanol of 63 ps.[8] The excited-state lifetime in sodium dodecylbenzyene-sulfonate/methanol medium is longer and found to be 109 ps.[15] In this work, we observed that the excited-state absorption and the stimulated emission decay of free alizarin in ethanol could be fitted mainly by one exponential with a time constant of 77 ps. In agreement with our previous investigation[8] only in the region of the isobestic point, where stimulated emission compensates excited-state absorption, a small contribution from a faster process with a time constant of 1.5 ps has been observed. This component was assigned to vibrational cooling within the excited electronic state of the dye.[8]

In contrast to that of the dye in ethanol, the dynamics observed for alizarin in the ethanol−water mixture could not be fitted with one exponential. A satisfactory description can only be achieved with at least three exponential components. The amplitude spectra obtained from the fitting analysis for the experimental data on alizarin/TiO_2 are shown in Figure 3. From the spectral characteristics the amplitude spectrum with the time constant 1.9 ps can be associated with the excited-state dynamics of the neutral alizarin form. Interestingly, the two other components are symmetric with respect to the *x* axis. This is a typical sign for the population and successive depopulation of a certain electronic state. The possible assignment of these additional time constants will be discussed in the subsequent section.

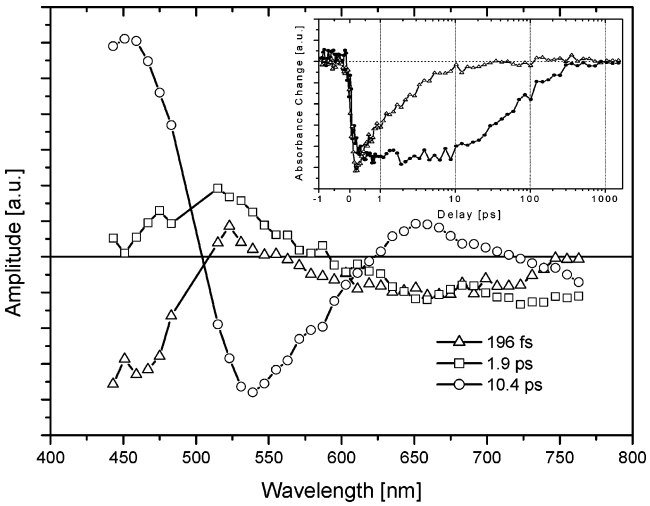

Figure 3. Amplitude spectra obtained from the global fitting analysis of experimental transient absorbance data for free alizarin in an ethanol−water mixture at pH 9. Inset: Transient absorbance kinetics of free alizarin in an ethanol−water mixture at pH 9 (△) and alizarin in ethanol (●) probed at $\lambda_{pr} = 731$ nm.

Transient Absorbance Measurements of Alizarin Coupled to the TiO_2 Nanoparticle Surface. We have performed transient absorbance investigations for the alizarin/TiO_2 coupled system in water−ethanol mixtures at pH 2 and 9. The transients were obtained after excitation at 500 nm and probed with spectrally broad white light. Because of the very strong electronic coupling between the dye and the semiconductor nanoparticle, an ultrafast forward electron transfer takes place in samples at investigated pH values. Within the resolution of the used experimental setup (~70 fs) we were not able to obtain a precise characteristic time constant and to resolve any possible changes of forward ET dynamics as a function of solvent pH. However, the time constant of injection of 6 fs for alizarin/TiO_2 in acidic solution was determined in earlier work,[8] and it is sufficient to assume that FET in the pH region from 2 to 9 was faster than 100 fs, since all further discussion and conclusions will be concentrated on the BET dynamics.

Since the BET dynamics of the alizarin-sensitized TiO_2 system in acidic water solution has already been the subject of several transient absorbance investigations,[8,10,15] here we will not concentrate on the description of the results obtained for alizarin/TiO_2 at pH 2. In brief, the transient absorbance spectra mainly consist of the dye ground-state bleach in the wavelength region between 450 and 590 nm and broad featureless positive absorption changes from 600 to 750 nm with a peak at 610 nm. The latter contribution can be assigned to the absorption of the injected electron itself,[8,28,46] while the absorption peak at 610 nm originates from the alizarin radical cation.[8,9]

Three selected, normalized transients for the alizarin-sensitized TiO_2 system at pH 2 and 9 probed at 523 nm (region of the ground-state bleach), 635 nm (alizarin cation absorption), and 723 nm (injected electron absorption) are given in Figure 4. Obviously, the temporal evolution of the transients in Figure 4 changes with the pH value. With increasing solution pH an additional component at probe wavelengths of $\lambda_{pr} = 635$ and 723 nm appears; it has negative absorption, which competes

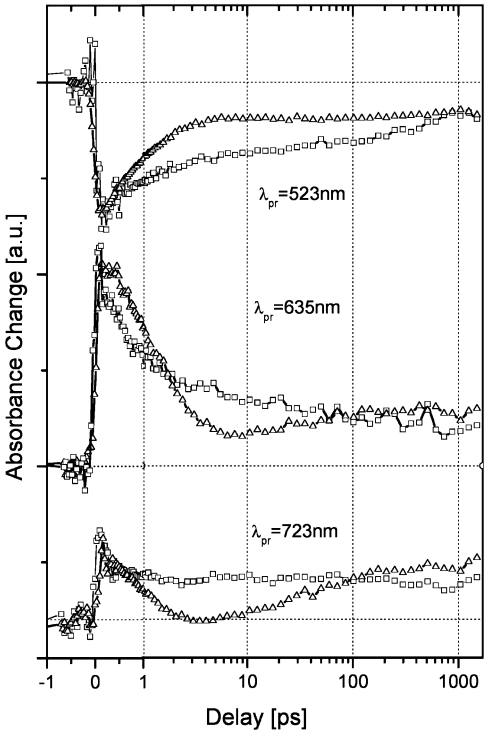

Figure 4. Transient absorbance kinetics of alizarin/TiO_2 at selected wavelengths: (△) pH 9, (□) pH 2.

with absorption of the injected electrons and persists for ~30 ps. One can also observe faster decay of the ground-state bleach at $\lambda_{pr} = 523$ nm and the alizarin cation absorption at $\lambda_{pr} = 635$ nm. It is necessary to note that residual signals remain at long delay times ($t_D > 1.5$ ns) for both pH values. This means that the charge-separated state after photoinduced injection is present in our experiments for at least nanoseconds in the pH range 2−9.

In the following sections the amplitude spectra of the alizarin-sensitized TiO_2 system at the pH values 2 and 9 will be described in detail. It should be noted that the signal-to-noise ratio of the data and thus the quality of the amplitude spectra in the regions of $\lambda_{pr} \approx 500$ nm and $\lambda_{pr} > 750$ nm for the alizarin/TiO_2 system (Figures 5 and 6) are reduced due to residual scattered light from the pump pulses ($\lambda_{pump} = 500$ nm) and the output from the laser/amplifier system ($\lambda_{CPA} = 775$ nm).

pH 2. The results of the global fitting analysis of the data for alizarin/TiO_2 at pH 2 are in very good agreement with the previously reported results.[8] A satisfactory fit of BET could be achieved with four time constants. Figure 5 shows the amplitude spectra of these time constants. From Figure 5 one can see that mostly two time constants ($\tau_1 = 240$ fs and $\tau_4 > 1.5$ ns) contribute in the absorption region of the injected electron ($\lambda_{pr} > 650$ nm). The two other spectra of the $\tau_2 = 2.6$ ps and $\tau_3 = 407$ ps components have their maxima at $\lambda_{pr} = 610$ nm and $\lambda_{pr} = 635$ nm, and their amplitudes are comparatively small at $\lambda_{pr} > 700$ nm, i.e., in the region where only the absorption of an electron in the conduction band is expected. Intuitively, the 2.6 and 407 ps time constants could be ascribed to recombination dynamics of the dye cation and the electrons from shallow and deep trap states, respectively.[8,27,47] On the other hand, all four time constants contribute significantly to the recovery of the ground-state bleach.

pH 9. A satisfactory description of the BET dynamics for alizarin/TiO_2 at pH 9 can be obtained with five time constants;

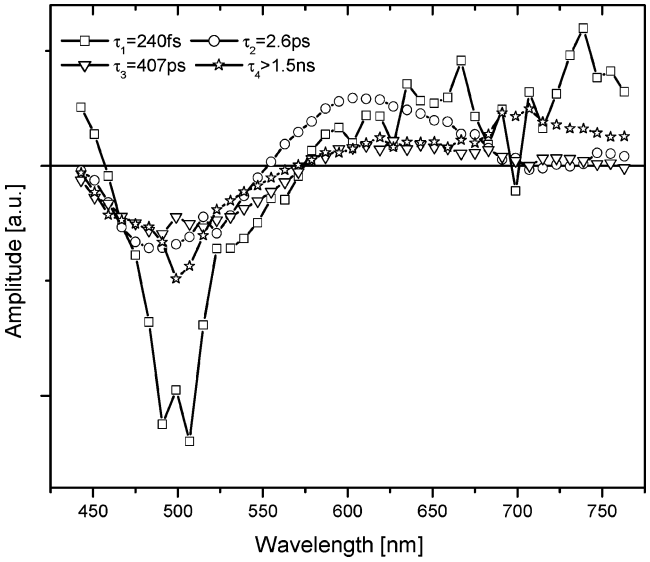

Figure 5. Amplitude spectra obtained from the global fitting analysis of experimental transient absorbance data for the alizarin/TiO_2 system at pH 2.

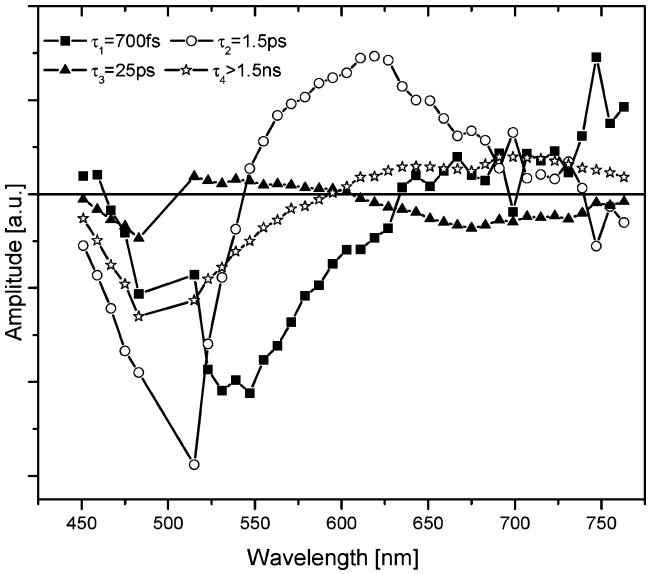

Figure 6. Amplitude spectra obtained from the global fitting analysis of experimental transient absorbance data for the alizarin/TiO_2 system at pH 9.

the four main components are shown in Figure 6. The amplitude spectra of the time constants $\tau_2 = 1.5$ ps and $\tau_4 > 1.5$ ns have spectral characteristics similar to those of the corresponding spectra for $\tau_2 = 2.6$ ps and $\tau_4 > 1.5$ ns at pH 2. From the similarity of the spectral features as well as the decay times these amplitude spectra could be ascribed to the same processes occurring in alizarin/TiO_2 at pH 9 and 2. However, three more exponentials were needed for complete fitting of the BET dynamics of the alizarin/TiO_2 system at pH 9. The amplitude spectrum for the $\tau_3 = 25$ ps component shows contributions in the region of the ground-state bleach with a minimum around $\lambda_{pr} = 490$ nm, in the region of the excited-state absorption (maximum at $\lambda_{pr} = 560$ nm), and also in the region of the stimulated emission (minimum at $\lambda_{pr} = 680$ nm). It is important to recognize its symmetry with regard to the *x* axis with the 700 fs time constant. The fifth time constant of $\tau_5 = 290$ ps (not shown in Figure 6) exhibits the smallest amplitude and can be preliminarily ascribed to the excited-state dynamics of

SCHEME 1: Schematic Energetics and Possible Dynamics for the Coupled Alizarin/TiO_2 System in Aqueous Solution at pH 2 (Left) and pH 9 (Right)

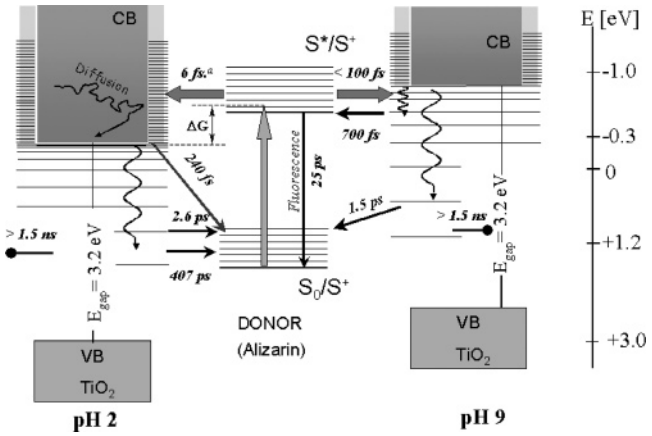

[a] An injection time of 6 fs for the alizarin/TiO_2 system in acidic solution has been measured by Huber et al.[9]

the alizarin monoanionic form coupled to the TiO_2 nanoparticle surface.

Discussion

Singlet Excited-State Dynamics of Free Alizarin. The evolution of the excited S_1 state of free alizarin has been subjected to several previous investigations.[8,15] Analysis of our data on alizarin in ethanol gives results which are consistent with the results reported in the previous studies. The excited-state lifetime can be determined from the evolution of the excited-state absorption and/or stimulated emission. Both processes decay in 77 ps, which is 14 ps longer than the lifetime reported for alizarin in methanol[8] and 32 ps shorter than the lifetime for the same dye in sodium dodecylbenzenesulfonate−methanol medium.[15]

In contrast to the results for alizarin in pure ethanol solution, the dye shows more complex dynamics in a water−ethanol mixture. As an example, the results of a transient absorbance analysis of alizarin in ethanol−water medium at pH 9 are presented in Figure 3. The amplitude spectrum for the time constant of 1.9 ps shows the relaxation of the excited state of the neutral alizarin form. The significant reduction of the excited-state lifetime (1.9 ps) of alizarin in water−ethanol solvent in comparison to alizarin in pure alcohol (77 ps) (see the inset of Figure 3) can be explained by intermolecular hydrogen bond formation with the aqueous solvent, which contributes in large part to the fast deactivation of the excited state.[40]

As has been mentioned before, alizarin in basic solution undergoes a deprotonation reaction. The time constant of 10.4 ps in Figure 3 with the largest amplitude shows the excited-state dynamics of the alizarin anion with contributions from excited-state absorption at $\lambda_{pr} = 460$ nm and the ground-state bleach at $\lambda_{pr} = 540$ nm. The symmetry of the amplitude spectra with characteristic times $\tau_1 = 196$ fs and $\tau_3 = 10.4$ ps with regard to the x axis indicates that population and successive depopulation of the anionic excited electronic state happen in the investigated system. Since the time constant $\tau_3 = 10.4$ ps has been assigned as a depopulation of the alizarin anion excited state, $\tau_1 = 196$ fs could be considered as a population time of this state which was initiated by photoexcitation. To explain this reaction pathway, the change of the acidity upon photoexcitation has to be taken into account. A large increase of alizarin acidity upon photoexcitation ($pK_1 - pK_1^* = 10$, where $pK_1 = 6.6$ and $pK_1^* = -3.4$) has been reported.[40] After excitation, the equilibrium between the neutral and the anionic alizarin form is disturbed and the formation of additional anions in the excited state with a typical time of $\tau_1 = 196$ fs can be observed. The acidochromic effects in alizarin and the possible steps of its deprotonation were described in detail by Miliani et al.[40]

Role of the Surface States for the pH Dependence of Interfacial Electron Transfer in the Alizarin/TiO_2 System. The main goal of this study is to investigate the pH dependence of interfacial electron transfer in the alizarin/TiO_2 coupled system, i.e., how the electron transfer depends on the energy of the participating electronic states. The conduction band position of TiO_2 is known to be pH-sensitive; changes of pH lead to a Nernstian shift of −59 mV/pH unit.[16,28−30] Furthermore, quantum-chemical calculations show that the alizarin photoexcited state is energetically located at the edge of the TiO_2 conduction band.[13] Thus, from the energetic situation it can be expected that relatively small changes of the solution pH should significantly affect the BET dynamics.

The BET dynamics for alizarin/TiO_2 for investigated pH values shows multiphasic kinetics with characteristic time constants from hundreds of femtoseconds to more than 1.5 ns. The wide range of time scales of BET dynamics is usually attributed to the different densities and natures of the trap states,[19,48,49] diffusion processes in the colloid,[50−52] and multiple injections per colloid.[48,53] The transient absorbance traces have been analyzed with a Marquardt downhill algorithm, where at least four and five exponential functions were needed for a complete description of the data for the alizarin/TiO_2 coupled system at pH 2 and 9, respectively (see Figures 5 and 6). To understand the nature of the trap states involved in BET processes, one has to consider in detail the amplitude spectra depicted in Figures 5 and 6. In a previous investigation of alizarin-sensitized TiO_2 nanoparticles in acidic solution, Huber et al.[8] concluded that the observed reaction kinetics throughout the entire investigated temporal range (<1.5 ns) was dominated by the ground-state recombination, which was not completed during the experimental observation range. Our results for alizarin/TiO_2 at pH 2 are in excellent agreement with the results reported in ref 8. Although the BET characteristics change significantly with increasing pH from 2 to 9, some processes involved remain unaffected. The spectra of the $\tau > 1.5$ ns time constants matches nearly perfectly the corresponding amplitude spectrum for pH 2, indicating that also in basic solution (pH 9) part of the participating dye molecules end up in a long-lived charge-separated state. The 2.6 ps (pH 2) and 1.5 ps (pH 9) time constants can be assigned to a ground-state recombination between an electron in the shallow trap state and the alizarin cation.

An electron transfer from deep trap states to the alizarin cation might be a possible explanation for the time constant of $\tau_3 = 407$ ps. The long recombination dynamics of electrons from the deep trap states and alizarin cations can be explained by a low coupling strength of the BET reaction. Interestingly, these processes are not present in the alizarin/TiO_2 system in alkaline solution (pH 9).

Trapped electrons in nanocrystalline TiO_2 films are reported to have a broad absorption band with a peak around 770 nm.[54] In contrast to these investigations we did not observe the absorption of the trapped electron in our time-resolved experiments: the amplitude spectra of the time constants $\tau_2 = 2.6$ ps and $\tau_3 = 407$ ps in Figure 5 and $\tau_2 = 1.5$ ps in Figure 6, which we assigned to a ground-state recombination between the

electron in the shallow/deep states and alizarin cations, have nearly zero intensity at $\lambda_{pr} > 700$ nm. This discrepancy can be explained by the difference in the absorption coefficients for alizarin/TiO_2 and the electron in the conduction band. The extinction coefficient for the electron absorption at $\lambda_{pr} = 600$ nm of 1200 M^{-1} cm^{-1} [53,55] is more than 7 times smaller than the extinction coefficient of the alizarin/TiO_2 complex (8700 M^{-1} cm^{-1} at $\lambda_{pr} = 500$ nm).[8] Because of the low extinction coefficient of the electron in the conduction band, its contribution is not observed in the amplitude spectra with our experimentally obtained signal-to-noise ratio.

The other two components with characteristic times of 700 fs and 25 ps at pH 9 (Figure 6) have no analogue at pH 2 (Figure 5). The corresponding amplitude spectra are symmetric with regard to the *x* axis, and can thus be considered as successive population and depopulation of a certain electronic state.[8] We ascribe these time constants to the repopulation of the alizarin excited state during the first 700 fs and its subsequent decay to the ground state via stimulated emission ($\lambda > 600$ nm) within 25 ps. Interestingly, the amplitude spectra of the alizarin/TiO_2 coupled system (Figure 6) are similar to the amplitude spectra obtained for alizarine/ZrO_2 as reported in ref 8 (see Figure 12 in that paper). This fact supports the assumption of similar energetic situations of the alizarin-sensitized ZrO_2 nanoparticles and the alizarin/TiO_2 system at pH 9. The origin of the processes at alkaline pH with a characteristic time constant of 290 ps is still unclear. From its spectral features it might be ascribed to a depopulation of the excited state of the alizarin monoanionic form coupled to the TiO_2 nanoparticle surface.

On the basis of the previous discussion and taking into account results reported for alizarin/ZrO_2,[8] two reaction pathways of BET from the TiO_2 nanoparticle to the sensitizing dye alizarin at pH 9 can be identified from our transient absorbance measurements (see Scheme 1). First, after the injection into surface states and cooling therein ($\tau_c < 100$ fs),[8] electrons could be transferred directly from the trap state of the nanoparticle to the alizarin ground state (S_0) with a characteristic time of 1.5 ps. Some electrons which are trapped in states with weak electronic coupling to alizarin can stay in the semiconductor nanoparticle during the entire investigated temporal range (<1.5 ns), contributing to the observed long-lasting charge-separated state. The second pathway leads to reinjection ($\sim$700 fs) of the trapped electron from the nanoparticle into lower vibrational levels of the excited state of alizarin with subsequent transition from S* to S_0 accompanied by delayed fluorescence.

Finally, it is quite remarkable that the BET dynamics observed for alizarin/ZrO_2[8] can be mimicked by simple chemical changes of the solution pH, i.e., by varying the driving force of the reaction. This is especially interesting in the context of the pH independence of the BET dynamics observed for some metal complexes covalently bound to nanocrystalline TiO_2 surfaces.[29] Thus, the alizarin/TiO_2 system, where the molecular photoexcited state is at the edge of the conduction band,[13] is a promising system to further investigate the dependence of the interfacial electron transfer on the driving force of the reaction and the role of surface states in this process.

Conclusions

Time-resolved transient absorbance spectroscopy in the visible region has been applied to investigate the pH dependence of interfacial ET dynamics in alizarin/TiO_2 systems. Steady-state absorption studies have shown that alizarin forms a charge-transfer complex with TiO_2 colloids in the pH range from 2 to 9. Due to a strong electronic coupling between the dye and the semiconductor nanoparticles,[8,9,15] alizarin-sensitized TiO_2 exhibits a very fast electron injection ($\tau < 100$ fs) at both pH 2 and 9 values. The BET recombination dynamics shows multiphasic kinetics and strongly depends on the sample pH. The changes of the BET dynamics with changing pH have been explained by a Nernstian-type alteration of the semiconductor conduction band edge position. By comparing the results of time-resolved experiments for alizarin/TiO_2 at pH 9 with the results obtained earlier for alizarin/ZrO_2,[8] we found that the differences between TiO_2 and ZrO_2 nanoparticles can be mimicked by a sole change in pH. Population, depopulation, and relaxation kinetics of a strongly coupled dye/semiconductor construct have been analyzed in detail, underlining the influence of surface trap states on interfacial electron transfer. Investigations on the pH dependence of the *forward* ET for strongly coupled dye/semiconductor systems with an experimental setup with improved temporal resolution are currently in progress in our laboratory.

Additionally, we have investigated the excited-state dynamics of free alizarin in ethanol and in a water−ethanol (4:1, v/v) mixture. The significant decrease of the excited-state lifetime in the water−ethanol mixture at pH 9 in comparison to that of alizarin in ethanol has been attributed to intramolecular hydrogen bond formation with the aqueous solvent, which promotes the fast deactivation of the excited state. Moreover, an ultrafast formation of monoanions in the excited state of alizarin in ethanol−water at pH 9 has been observed. This finding explains the results obtained by time-resolved transient absorbance spectroscopy.

Acknowledgment. This work is supported by the Deutsche Forschungsgemeinschaft (DFG; Grant WA 1012/2-1). We thank Dr. M. Grätzel and Dr. J. E. Moser (Ecole Polytechnique Fédérale de Lausanne, Switzerland) for providing us with the nanoparticle samples and Dr. A. Dreuw for helpful discussions.

References and Notes

(1) Wu, T. X.; Liu, G. M.; Zhao, J. C.; Hidaka, H.; Serpone, N. *J. Phys. Chem. B* **1999**, *103*, 4862.
(2) Oregan, B.; Grätzel, M. *Nature* **1991**, *353*, 737.
(3) Bach, U.; Lupo, D.; Comte, P.; Moser, J. E.; Weissortel, F.; Salbeck, J.; Spreitzer, H.; Grätzel, M. *Nature* **1998**, *395*, 583.
(4) Nitzan, A.; Ratner, M. A. *Science* **2003**, *300*, 1384.
(5) Moser, J.; Grätzel, M. *J. Am. Chem. Soc.* **1984**, *106*, 6557.
(6) Moser, J.; Grätzel, M.; Sharma, D. K.; Serpone, N. *Helv. Chim. Acta* **1985**, *68*, 1686.
(7) Ghosh, H. N.; Asbury, J. B.; Weng, Y. X.; Lian, T. Q. *J. Phys. Chem. B* **1998**, *102*, 10208.
(8) Huber, R.; Spörlein, S.; Moser, J. E.; Grätzel, M.; Wachtveitl, J. *J. Phys. Chem. B* **2000**, *104*, 8995.
(9) Huber, R.; Moser, J. E.; Grätzel, M.; Wachtveitl, J. *J. Phys. Chem. B* **2002**, *106*, 6494.
(10) Huber, R.; Moser, J. E.; Grätzel, M.; Wachtveitl, J. *Chem. Phys.* **2002**, *285*, 39.
(11) Anderson, N. A.; Lian, T. Q. *Annu. Rev. Phys. Chem.* **2005**, *56*, 491.
(12) Ai, X.; Anderson, N. A.; Guo, J. C.; Lian, T. Q. *J. Phys. Chem. B* **2005**, *109*, 7088.
(13) Duncan, W. R.; Stier, W. M.; Prezhdo, O. V. *J. Am. Chem. Soc.* **2005**, *127*, 7941.
(14) Ramakrishna, G.; Das, A.; Ghosh, H. N. *Langmuir* **2004**, *20*, 1430.
(15) Ramakrishna, G.; Singh, A. K.; Palit, D. K.; Ghosh, H. N. *J. Phys. Chem. B* **2004**, *108*, 1701.
(16) Moser, J. E.; Grätzel, M. *Chem. Phys.* **1993**, *176*, 493.
(17) Tachibana, Y.; Moser, J. E.; Grätzel, M.; Klug, D. R.; Durrant, J. R. *J. Phys. Chem.* **1996**, *100*, 20056.
(18) Hao, E. C.; Anderson, N. A.; Asbury, J. B.; Lian, T. Q. *J. Phys. Chem. B* **2002**, *106*, 10191.
(19) Barzykin, A. V.; Tachiya, M. *J. Phys. Chem. B* **2002**, *106*, 4356.
(20) Marcus, R. A. *J. Chem. Phys.* **1965**, *43*, 679.
(21) Marcus, R. A.; Sutin, N. *Biochim. Biophys. Acta* **1985**, *811*, 265.
(22) Gao, Y. Q.; Marcus, R. A. *J. Chem. Phys.* **2000**, *113*, 6351.

(23) Gosavi, S.; Marcus, R. A. *J. Phys. Chem. B* **2000**, *104*, 2067.
(24) Gao, Y. Q.; Georgievskii, Y.; Marcus, R. A. *J. Chem. Phys.* **2000**, *112*, 3358.
(25) Ellingson, R. J.; Asbury, J. B.; Ferrere, S.; Ghosh, H. N.; Sprague, J. R.; Lian, T. Q.; Nozik, A. J. *J. Phys. Chem. B* **1998**, *102*, 6455.
(26) Olsen, C. M.; Waterland, M. R.; Kelley, D. F. *J. Phys. Chem. B* **2002**, *106*, 6211.
(27) Rath, M. C.; Ramakrishna, G.; Mukherjee, T.; Ghosh, H. N. *J. Phys. Chem. B* **2005**, *109*, 20485.
(28) Duonghong, D.; Ramsden, J.; Grätzel, M. *J. Am. Chem. Soc.* **1982**, *104*, 2977.
(29) Yan, S. G.; Hupp, J. T. *J. Phys. Chem.* **1996**, *100*, 6867.
(30) Gaal, D. A.; Hupp, J. T. *J. Am. Chem. Soc.* **2000**, *122*, 10956.
(31) Zaban, A.; Ferrere, S.; Gregg, B. A. *J. Phys. Chem. B* **1998**, *102*, 452.
(32) Zaban, A.; Ferrere, S.; Sprague, J.; Gregg, B. A. *J. Phys. Chem. B* **1997**, *101*, 55.
(33) Yan, S. G.; Hupp, J. T. *J. Phys. Chem. B* **1997**, *101*, 1493.
(34) Duncan, W. R.; Prezhdo, O. V. *J. Phys. Chem. B* **2005**, *109*, 365.
(35) Moser, J.; Grätzel, M. *J. Am. Chem. Soc.* **1983**, *105*, 6547.
(36) Huber, R.; Kohler, T.; Lenz, M. O.; Bamberg, E.; Kalmbach, R.; Engelhard, M.; Wachtveitl, J. *Biochemistry* **2005**, *44*, 1800.
(37) Helbing, J.; Bregy, H.; Bredenbeck, J.; Pfister, R.; Hamm, P.; Huber, R.; Wachtveitl, J.; De Vico, L.; Olivucci, M. *J. Am. Chem. Soc.* **2004**, *126*, 8823.
(38) Wilhelm, T.; Piel, J.; Riedle, E. *Opt. Lett.* **1997**, *22*, 1494.
(39) Huber, R.; Satzger, H.; Zinth, W.; Wachtveitl, J. *Opt. Commun.* **2001**, *194*, 443.
(40) Miliani, C.; Romani, A.; Favaro, G. *J. Phys. Org. Chem.* **2000**, *13*, 141.
(41) Miliani, C.; Romani, A.; Favaro, G. *Spectrochim. Acta, Part A* **1998**, *54*, 581.
(42) Smith, T. P.; Zaklika, K. A.; Thakur, K.; Barbara, P. F. *J. Am. Chem. Soc.* **1991**, *113*, 4035.
(43) Smith, T. P.; Zaklika, K. A.; Thakur, K.; Walker, G. C.; Tominaga, K.; Barbara, P. F. *J. Phys. Chem.* **1991**, *95*, 10465.
(44) Rajh, T.; Chen, L. X.; Lukas, K.; Liu, T.; Thurnauer, M. C.; Tiede, D. M. *J. Phys. Chem. B* **2002**, *106*, 10543.
(45) Palomares, E.; Vilar, R.; Green, A.; Durrant, J. R. *Adv. Funct. Mater.* **2004**, *14*, 111.
(46) Furube, A.; Asahi, T.; Masuhara, H.; Yamashita, H.; Anpo, M. *J. Phys. Chem. B* **1999**, *103*, 3120.
(47) Zhang, J. Z. *J. Phys. Chem. B* **2000**, *104*, 7239.
(48) Haque, S. A.; Tachibana, Y.; Willis, R. L.; Moser, J. E.; Grätzel, M.; Klug, D. R.; Durrant, J. R. *J. Phys. Chem. B* **2000**, *104*, 538.
(49) Huang, S. Y.; Schlichthorl, G.; Nozik, A. J.; Grätzel, M.; Frank, A. J. *J. Phys. Chem. B* **1997**, *101*, 2576.
(50) Lindstrom, H.; Rensmo, H.; Sodergren, S.; Solbrand, A.; Lindquist, S. E. *J. Phys. Chem.* **1996**, *100*, 3084.
(51) Solbrand, A.; Henningsson, A.; Sodergren, S.; Lindstrom, H.; Hagfeldt, A.; Lindquist, S. E. *J. Phys. Chem. B* **1999**, *103*, 1078.
(52) Usami, A. *Chem. Phys. Lett.* **1998**, *292*, 223.
(53) Rothenberger, G.; Moser, J.; Grätzel, M.; Serpone, N.; Sharma, D. K. *J. Am. Chem. Soc.* **1985**, *107*, 8054.
(54) Yoshihara, T.; Katoh, R.; Furube, A.; Tamaki, Y.; Murai, M.; Hara, K.; Murata, S.; Arakawa, H.; Tachiya, M. *J. Phys. Chem. B* **2004**, *108*, 3817.
(55) Kolle, U.; Moser, J.; Grätzel, M. *Inorg. Chem.* **1985**, *24*, 2253.